Spectroscopic study on relationship between contacts erosion and chromatic parameters of arc in a HVCB

Zhixiang Wang[1,2], Gordon R. Jones[2], Joseph W. Spencer[2], Xiaohua Wang[1], Mingzhe Rong[1]

[1]Xi'an Jiaotong University, State Key Laboratory of Electrical Insulation for Power Equipment, School of Electrical Engineering, 28 Xianning West Rd, Xi'an, 710049, China
[2]University of Liverpool, Brownlow Hill, Liverpool, L69 3GJ, UK

E-mail: wangzhixiang.215@gmail.com

November 2016

Abstract. Contacts erosion is one of the most crucial factor affecting the electrical service lifetime of high-voltage circuit breakers (HVCBs). Monitoring the contacts' erosion degree is increasingly in demand for the sake of condition based maintenance to guarantee the functional operation of HVCBs. An experimental test rig has been designed based upon a commercial 245kV/40kA SF_6 puffer type circuit breaker with copper-tungsten (28%wt and 72%wt) arcing contacts under atmospheric pressure. Three optical-fibre based sensors are used to capture the time-resolved spectra of arcs. A novel approach using chromatic methods to process the time-resolved spectral signal has been proposed. The processed chromatic parameters have been interpreted to show that the time variation of spectral emission from the contact material and quenching gas are closely correlated to the mass loss and surface degradation of the plug arcing contact. The feasibility of applying this method to on-line monitoring of contact erosion is indicated.

Keywords: contacts erosion, HVCB, chromatic methods, spectroscopic

1. Introduction

Contacts erosion in high-voltage circuit breakers (HVCBs) is an inevitable consequence of current interruption and is caused primarily by vaporisation and splashing of molten material of the electrodes. The mass loss and surface structure changing of arcing contacts adversely affects the interruption performance of HVCBs and therefore determines their electrical service lifetime[1].

To avoid unexpected current interruption failure and save maintenance cost, on-line monitoring of arcing contacts is increasingly in demand. So far, the prediction of mass loss and maintenance of arcing contacts are mainly based on empirical knowledge or accumulations of breaking current and arcing time[2]. Over the past decades, several investigations have been undertaken to study the arcing contacts erosion[3, 4, 5, 6, 7]. Generally, conclusions are drawn according to the energy balance at the arc-electrode interface without considering practical changes which might have occurred in the contact geometry and surface morphology. Therefore, there may be deficiencies in the predictions made with these models for practical applications.

An aim of this investigation is to seek a measurable parameter which has direct correlation with the mass loss of an arcing contact. It is not feasible to measure directly contact erosion in an in service HVCB, but optical emissions from the arc may contain relevant contact information and may be conveniently monitored. Such information is manifest in the spectra of such optical signals, so that an approach of correlating mass loss of an arcing contact with such arc spectra is proposed.

However a flexible and effective data processing method is needed to extract useful information from the complex spectral emissions. Therefore, a chromatic method was selected for addressing the complex spectra. This method is a hierarchical approach used for dimensionality reduction, feature detection and cluster analysis which is suitable for on-line condition monitoring[8]. It offers the possibility for distinguishing changes in a system and for traceing the reasons for the changes without recourse to the need for detailed scientific calculations which may be suspect to noise interferences.

This contribution describes an experimental setup for monitoring contact erosion, followed by some typical results. Thereafter, the deployment of chromatic data processing methods is described and the correlation between contacts erosion and chromatic parameters discussed.

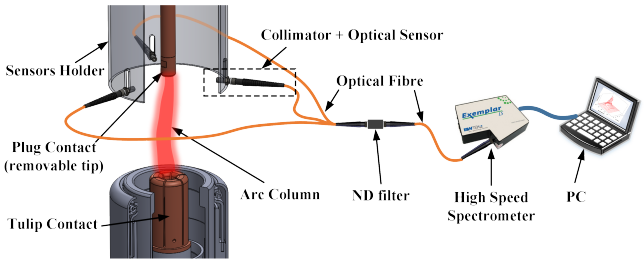

Figure 1. Schematic Diagram of Interrupter and optical measurement system.

2. Experimental Test System

2.1. Circuit Breaker Unit

A schematic diagram of the current interrupter unit used for the present tests is shown on figure 1. This unit represented a commercial 245kV/40kA (RMS) live tank puffer type SF_6 HVCB[9] operating at a pressure of 1bar. The material of the contacts was copper/tungsten (28wt% of copper and 72wt% of tungsten). The plug contact was attached to the top plate of the unit and its diameter was 18mm. The contact tip was redesigned to be removable so that the mass loss could be measured by weighing before and after each operation with an electronic balance (Sartorius Master^{pro} Series LP1200S) whose precision was 1mg. The moving contact was connected to a driving mechanism for opening the contact gap whose maximum opening speed was 5m/s. The fully opened gap was approximately 100mm. The plug contact was used as the cathode and the tulip contact as the anode. Only the erosion of the plug contact was investigated. The main interrupter nozzle was removed to avoid the erosion process being affected by a possible interaction between the arc and the PTFE nozzle material.

2.2. Optical System

The optical system used for monitoring the spectral emission from an arc (figure1) was composed of three optical sensors which were installed at the same height as the plug contact surface and set at 120 degrees to each other. The observation area covered by each sensor was adjusted by a collimator to correspond to the contact diameter at the symmetry axis. Thus the light emission from the arc could be captured equally by three sensors via a single channel rapid response spectrometer (Exemplar LS, spectral resolution of 0.6nm, minimum integration time 1050us, maximum data transfer speed 950 spectra per second via USB3.0 cable). Approximately 10 spectra could be recorded during a half cycle arcing period of ∼10ms. Since the absolute radiative energy from the arc was intense, before the optical light was fed into the spectrometer,

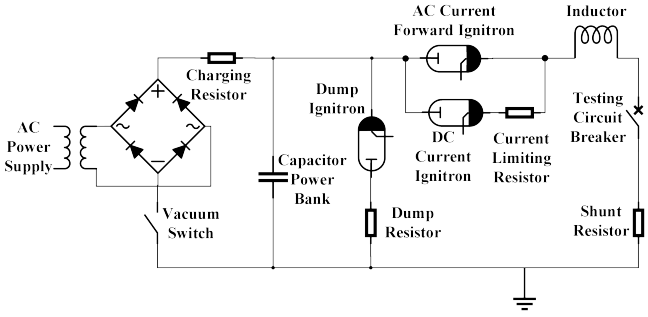

Figure 2. Schematic diagram of test circuit.

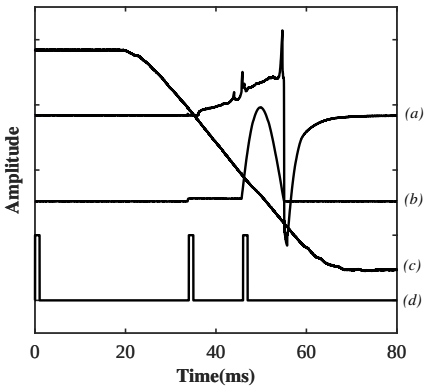

Figure 3. Experimental timing sequence and typical waveforms: (a) arc voltage, (b) arc current, (c) contacts separation (d) trigger signals.

an adjustable neutral density (ND) filter was used to avoid saturation and the raw data was compensated before processing.

2.3. Power Test Circuit

A capacitor/inductor resonance circuit (figure 2) was used to generate a half cycle of alternating current. The main capacitor, used as the power source, had a capacitance of 35mF, a maximum charging voltage of 6.3kV and a maximum energy stored of 695kJ. To provide a resonant current of 60Hz, an inductance of 184μH was connected in series with the capacitor bank. The capacitor charging system consisted of a transformer, rectifier, vacuum switch and charging resistor. A DC ignitron was installed to produce an arc initiation current through a current limiting resistor. This provided a low level direct current prior to an ignitron switching it to the AC current with an AC ignitron. A dump ignitron and resistor were installed to discharge the capacitor bank for safety reasons with precise timing as determined by the experiments. The current and voltage of the arc were measured with a shunt resistor of 1.19mΩ and a high voltage probe (Tek P6015A) respectively. Trigger pulses required by the ignitrons were generated by the main control unit (MCU).

2.4. Test Procedures

Some typical time varying waveforms for (a) arc voltage, (b) arc current, (c) contact travel and (d) trigger pulses are shown in figure 3. A test was initiated by a "main trigger" at time zero. The main trigger was sent to the oscilloscope, spectrometer and also the circuit breaker operating mechanism. The tulip contact (figure 1) started to move after approximately 20ms after the initiation pulse (figure 3). Thereafter, a second trigger pulse initiated a low level DC current (∼several hundred amperes) prior to the moment of contacts separation in order to initialise the arcing and keep the gap between the two contacts conducting. After a fixed period of time, a third trigger was sent to initiate the positive half cycle of AC current lasted for from 46ms until 56ms (figure 3). The displacement curve of the moving contact (figure 3 (c)) was also recorded using a linear position transducer. The timing sequence from test to test was highly repeatable.

Table 1. Assignment of test numbers.

Test Current	1st	2nd	3rd	4th	5th
5kA	a1	a2	a3	a4	a5
10kA	b1	b2	b3	b4	b5
15kA	c1	c2	c3	c4	c5
20kA	d1	d2	d3	d4	d5
25kA	e1	e2	e3	e4	e5
30kA	f1	f2	f3	f4	f5
35kA	g1	g2	g3	g4	g5
40kA	h1	h2	h3	h4	h5

Eight different peak current levels were used, namely 5kA$_p$, 10kA$_p$, 15kA$_p$, 20kA$_p$, 25kA$_p$, 30kA$_p$, 35kA$_p$ and 40kA$_p$ (Table 1). For each current level, five tests were performed each with a new plug contact tip. The circuit breaker arcing chamber was opened after each single test so that the individual mass loss of the plug contact could be obtained. This enabled the relationship between contact mass loss and optical signature from the optical monitoring system to be studied. A unique test number was assigned to each of these tests as shown in Table 1.

3. Experimental Results

3.1. Mass Loss from Contact Weight Measurements

Figure 4 shows the measured mass loss of the plug contact after each test as a function of peak current. The color bar shows the progression of increasing mass loss from white (bright) to red (dark). The test number is shown at the centre of each point.

The graph shows that the variation of the mass

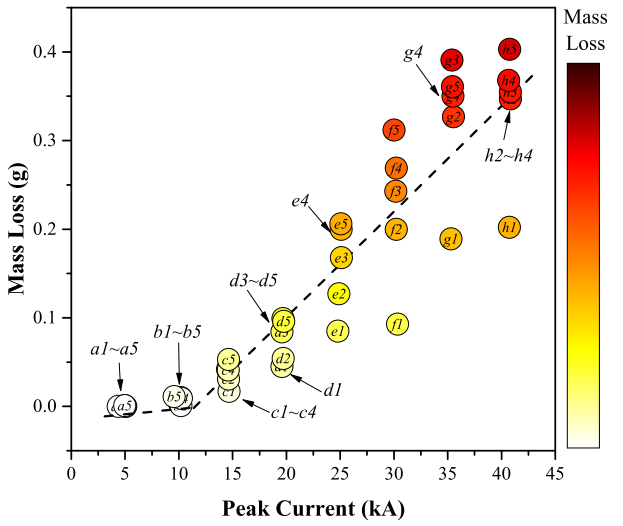

Figure 4. Measured mass loss of plug contact as function of peak current

loss with peak current was non-linear with an inflection point occurring between 10kA to 15kA. From 5kA to 10kA, the mass loss was relatively low because the absolute energy flux input into the contact was weak and the movement of the arc spot on the contact dissipated the energy at various locations along the contact surface[10]. Therefore, the energy available for heating and eroding the contact material was limited. From 15kA up to 40kA, a decrease in the arc spot mobility has been observed[10]. This produced more energy at selected fixed locations on the contact surface leading to increased temperatures and hence a higher rate of contact erosion. Such a discontinuous contact erosion rate as a function of increasing current has also been reported by other researchers[5, 11, 4].

For the same current levels, the mass loss rate generally increased with test numbers. This was especially so for the first test on a new contact, the mass loss being remarkably lower than those of subsequent tests. This effect was more pronounced at high current levels.

Since the erosion rate of an individual breaking operation at 'low' current levels is quite small compared to the accuracy of the mass loss measurements, only the test results over 15kA peak (inclusive) are considered. Apart from the mass loss, images of the plug contact tips were also taken (figure 5) to provide more evidence about the mechanisms of contact erosion.

3.2. Time Varying Spectra

An example of a typical time varying spectra is shown in figure 6. Strong emissions can be observed in the range from 500nm to 550nm. Emissions from Copper(Cu), Tungsten(W) and Sulphur(S) are listed

Figure 5. Contact surface images for different peak arc currents (a) 5kA, first test a1 (b) 25kA, first test e1 (c) 40kA, fifth test h5.

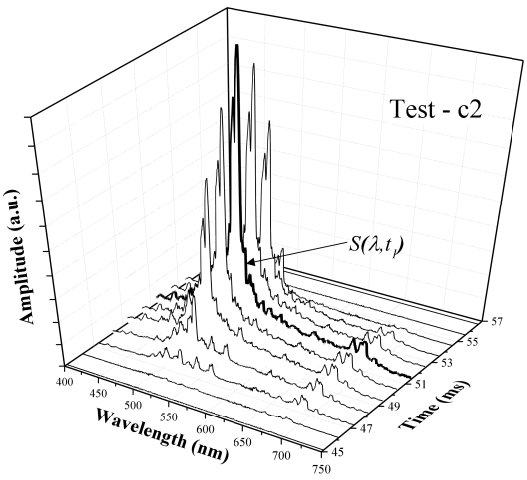

Figure 6. A typical time-resolved spectral signal.

Table 2. Strong emission lines of tungsten, copper and sulfur in visible spectrum range [12].

Elements	Strong Emission Lines (nm)
W I	400.9, 407.4, 429.5, 430.2, 448.4 465.9, 468.1, 484.4
Cu I	510.6, 515.3, 521.8
S II	542.9, 543.3, 545.4, 547.4, 551.0 560.6, 564.0

on Table 2. The spectra and their time variation are clearly complex.

4. Analysis of Test Results

4.1. Chromatic Techniques

The complex, time varying, optical spectra (figure 6) have been analysed using chromatic processing techniques. This approach involves addressing a complex signal with three non-orthogonal processors (R, G, B)[13] (figure 7) which are used to quantify various signal features such as the effective signal strength (L), relative magnitudes of three signal

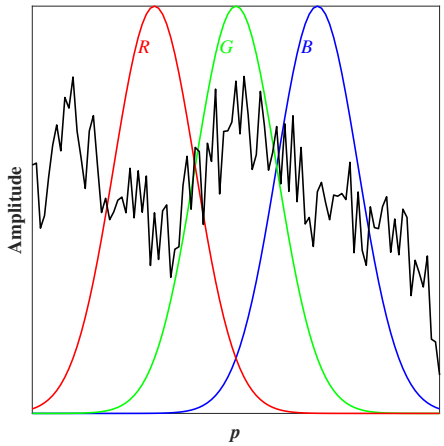

Figure 7. Schematic diagram of tri-stimulus chromatic processors (R, G, B) superimposed upon a complex signal $S(p)$ as a function of a parameter p.

distribution components (x, y, z) which are defined by the following equations[13]

$$L = (R + G + B)/3 \quad (1)$$

$$x = R/3L; \quad y = G/3L; \quad z = B/3L \quad (2)$$

A signal may then be defined by its x, y, z coordinates as a single point on a two dimensional x, y, z chromatic map[13]. Additionally, trends in signal changes may be represented by values of x, y, z as a function of factors producing the signal changes.

4.2. Primary Chromatic Analysis

A primary chromatic analysis was undertaken of the arc spectral emission at the peak value (t_1, figure 6) of each of the currents investigated (Table 1). An example of the deployment of three chromatic processors (R_w, G_w, B_w) for addressing such a wavelength spectrum is shown on figure 8. The responses of the three processors covered the wavelength ranges occupied by the emission bands of tungsten (W I), Copper (Cu I), Sulphur (S II) (Table 2). The outputs from the three processors (R_w, G_w, B_w) were converted into three primary chromatic parameters $x_w(t_1)$, $y_w(t_1)$ and $z_w(t_1)$ using equations (1) and (2).

Values of the primary chromatic parameters $y_w(t_1)$ and $z_w(t_1)$ were plotted against the directly measured mass loss (figure 4) to yield trend results shown on figures 9(a) and 9(b) respectively.

4.3. Secondary Chromatic Parameters

Primary Chromatic Parameters at various times (t) during a current half cycle ($x_w(t)$, $y_w(t)$, $z_w(t)$) were also calculated and the time variation of each during a half cycle was addressed by three time

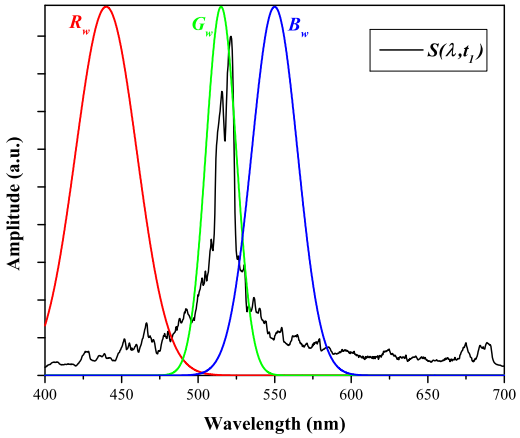

Figure 8. Wavelength domain processors R_w, G_w, B_w superimposed upon a typical arc spectrum.

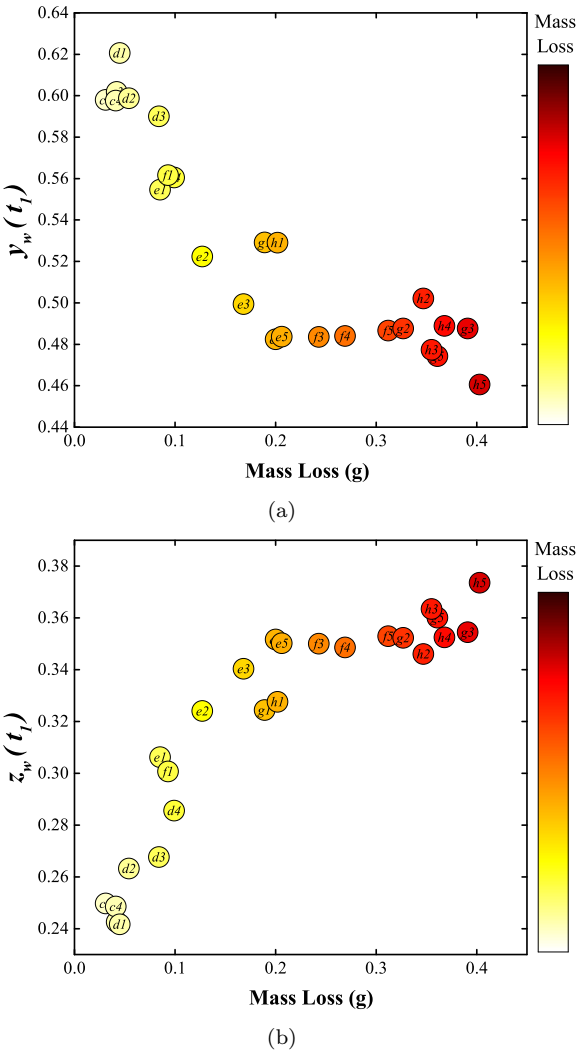

Figure 9. Primary chromatic parameters as functions of mass loss. (a) $y_w(t_1)$ (b) $z_w(t_1)$.

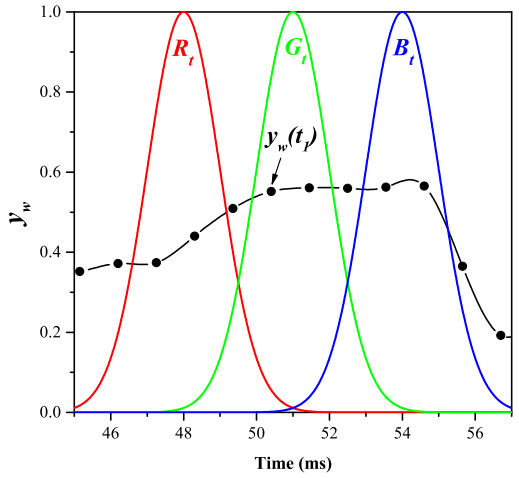

Figure 10. Example of time domain chromatic processors R_t, G_t, B_t superimposed upon the time variation of wavelength chromatic parameter y_w $(= G_{w0}/(R_{w0} + G_{w0} + B_{w0}))$.

Table 3. List of all secondary chromatic parameters.

Wavelength\Time	x_t	y_t	z_t
$x_w(t)$	x_{txw}	y_{txw}	z_{txw}
$y_w(t)$	x_{tyw}	y_{tyw}	z_{tyw}
$z_w(t)$	x_{tzw}	y_{tzw}	z_{tzw}

domain chromatic parameters (R_t, G_t, B_t). An example of the time variation of the primary chromatic (wavelength domain) parameter ($y_w(t)$) is shown on figure 10 along with the three time domain chromatic processors superimposed. Nine Secondary Chromatic (time domain) Parameters (e.g. y_{tyw} and y_{tzw} etc., Table 3) were evaluated from the R_t, G_t, B_t outputs.

The variation of each of two of these nine parameters (y_{tyw} and y_{tzw}) with directly measured contact mass loss (figure 4) is shown on figure 11(a) and 11(b).

Figure 12 shows a Secondary Chromatic Map of y_{tyw} versus y_{tzw} from which a clear mass loss trend can be conveniently visualised.

5. Discussion

The Primary Chromatic Parameters $y_w(t_1)$, $z_w(t_1)$ shown in figure 9(a) and 9(b) represent the relative emission from the CuI and SII bands respectively at t_1. Figure 9(a) shows that with increasing mass loss $y_w(t_1)$ generally decreased indicating that the relative emission from CuI band at t_1 became less pronounced. By contrast, $z_w(t_1)$ increased with mass loss indicating that the relative emission from SII (i.e. the surrounding gas) was becoming stronger. However, the relationships between each of these

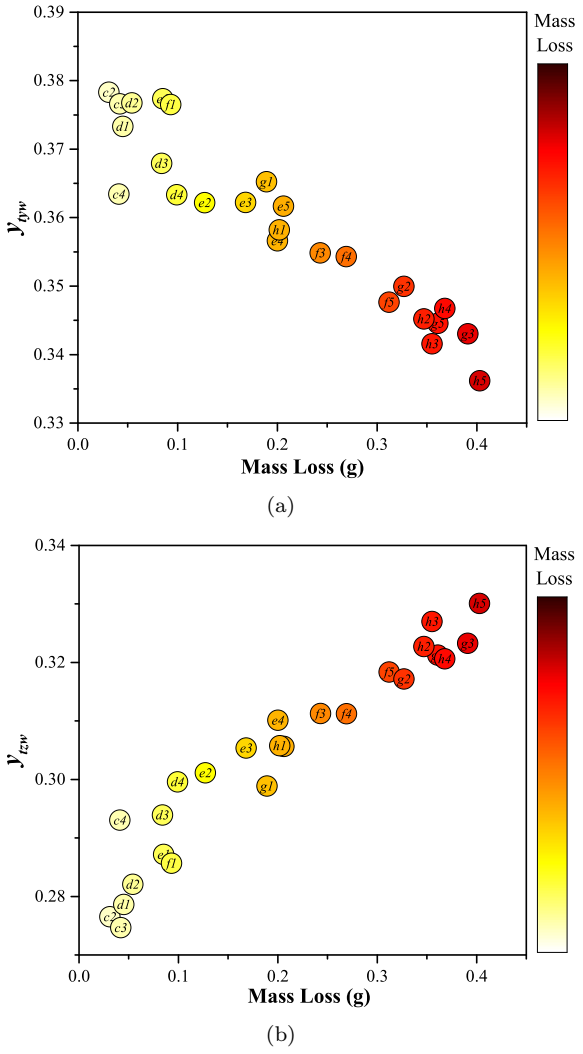

Figure 11. Secondary chromatic parameters as a function of mass loss. (a) y_{tyw} (b) y_{tzw}.

primary chromatic parameters and mass loss are not monotonic particularly when the mass loss is higher than 0.2g. As such there is a loss of sensitivity for determining mass loss level in this range and recourse may be made to examining possibilities with Secondary (time domain) Chromatic Processing.

Figure 11(a) and figure 11(b) show that two selected Secondary Chromatic Parameter y_{tyw} and y_{tzw} both varied monotonically with increasing contact mass loss and only moderate scatter. As such and with further testing they have a potential for being utilized for mass loss prediction.

The secondary parameter y_{tyw} represents the magnitude during the medium time period (peak current)(i.e. G_t, figure 10) relative to the other time periods of the relative emission from the CuI band (G_w, figure 8). The decrease in the value of y_{tyw} with increasing mass loss may be explained as follows. Due

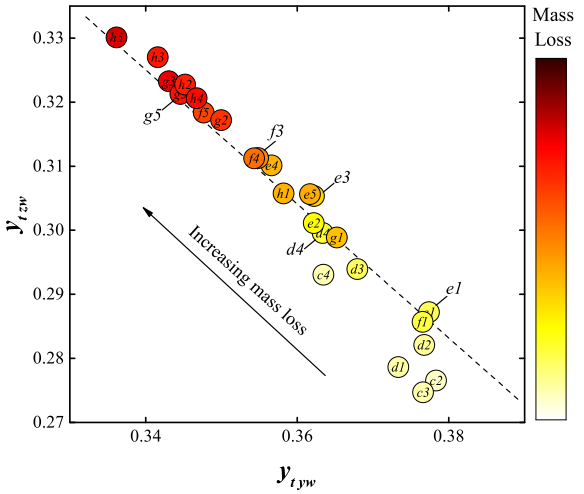

Figure 12. Secondary chromatic parameter map of y_{tyw} vs y_{tzw}.

to insufficient heating at the contact surface at 'low' current levels, the emission peak from the CuI band coincided with the current peak which occurred at the medium time period. Hence, the value of y_{tyw} at low current levels tended to be greater. As the current increased, the emission peak shifted to the later time period because of continuous intensive heating from the arc. Therefore, the value of z_{tyw} increased whilst that of y_{tyw} decayed. By contrast, the medium time period relative emission from SII band y_{tzw} showed an opposite trend with increasing mass loss. This trend suggested that the surrounding gas being heated so the emission from SII band (B_w, figure 8), was more intense during the peak current phase with growing mass loss.

The combination of y_{tyw} and y_{tzw} offered an enhanced prediction of mass loss as shown in figure 12.

The measured erosion mass versus peak current results of figure 4 shows the following:

- For peak currents < 15kA, the erosion is negligible and does not vary with repeated arcing (a1 → a2; b1 → b2, figure 4).
- For peak currents > 15kA, the erosion level is not negible at the first test and increases with successive tests (e.g. 25kA, e1 → e5, figure 4)

The chromatically analysed test results show the same trend as the direct measurements (figures 9, 11) whereas conventional estimates of the erosion level by integrating the arcing current with respect to time does not distinguish between the lower and higher currents behaviour.

Inspection of images of the contact after each successive test at a given peak current (figures 5(a), 5(b), 5(c)) suggests that the observed different behaviour at the lower (<15kA) and higher(>15kA) peak currents may be associated with different modes of contact wear.

At a low current of 5kA, the contact surface did not suffer a major change (figure 5(a)). However, after one test at a higher peak current of 25kA the contact surface was substantially changed (figure 5(b)) with re-solidified copper (brown) from the sintered copper/tungsten of the contact material indicating that due to the special properties of sintered copper/tungsten material[1] producing a layered structure. With an increase in peak current, more copper from deeper locations is melted and vaporized. After a few more tests on the same contact, especially for high current levels, the layered structure appeared to be formed with melted tungsten on the top, tungsten skeleton in the middle and copper/tungsten mixture at the bottom[14]. During the subsequent tests, the solid tungsten layer would be heated up to its melting temperature before the copper could be vaporized. This effect is consistent with the value of y_{tyw} deceasing during subsequent tests since the formation of the 'tungsten layer' delayed the appearance of CuI emission peak.

Thus the processed secondary chromatic parameters is not only capable of predicting the mass loss of a contact (after calibration), but can also indicate the changes in the structure of the contact surface.

6. Conclusions

Investigation have been reported about the erosion of a plug arcing contact in a HVCB subjected to a half cycle of current. Results of experiments with copper/tungsten arcing contacts subjected to current up to 40kA peak have been presented.

Mass loss from a contact following arcing have been measured for a) a range of peak arc currents b) repeated tests with the same contact and peak currents. The results of these tests show that there was a non-linear relationship between the mass loss of the plug contact and peak current with an inflection point occurring between 10kA to 15kA.

For each peak current level, the first test on a new contact tended to have a lower erosion rate than those of subsequent tests and this effect was more pronounced at high current levels.

Time-resolved spectra of the contact eroding arcs have been obtained and processed using chromatic methods. The mass loss was correlated with selected secondary chromatic parameters y_{tyw} and y_{tzw} and the following conclusions were obtained:

- As mass loss increased, the ratio of the emission from CuI band spectra around peak current decreased.

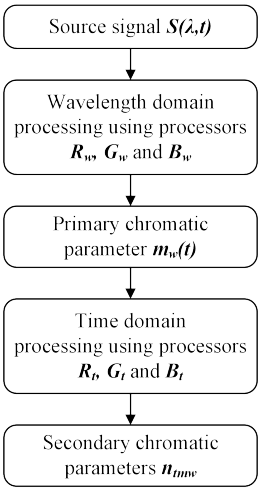

Figure 13. Flow chart for spectral data processing using chromatic methods (m ,n are x, y, z).

- The ratio of the emission from SII band spectra, showed an opposite trend to CuI, increasing around peak current.

The procedures followed to produce the chromatic results from the spectral data may be summarised by the flow chart given on figure 13.

Images of plug contacts exposed to different currents have been presented which show various changes in the surface topology of a contact. Conclusions have been drawn about the relationship between the current effect on surface topology and the mass losses plus chromatic trends.

It may be possible to derive additional information from different secondary chromatic parameters using other transformation algorithms (refer to book [13]). Moreover, the quantitative nature of the chromatic parameters can be used for on-line monitoring of contacts erosion. The influence of arcing time, polarity of current and nozzle ablation on high current contacts erosion and its arcing spectral signatures require further investigation.

Acknowledgement

This research has been supported by the China Scholarship Council, National Key Basic Research Program (973 Program) of China (No. 2015CB251001) and National Science Foundation of China (Grant No.51521065 and 51407136).

Reference

[1] J. Tepper, M. Seeger, T. Votteler, V. Behrens, and T. Honig, "Investigation on erosion of cu/w contacts in high-voltage circuit breakers," *Ieee Transactions on Components and Packaging Technologies*, vol. 29, no. 3, pp. 658–665, 2006.

[2] A. Poeltl and M. Haines, "Experiences with condition monitoring of hv circuit breakers," *2001 Ieee/Pes Transmission and Distribution Conference and Exposition, Vols 1 and 2*, pp. 1077–1082, 2001.

[3] R. Holm, "The vaporization of the cathode in the electric arc," *Journal of Applied Physics*, vol. 20, no. 7, pp. 715–716, 1949.

[4] H. W. Turner and C. Turner, "Choosing contact materials," *Electronics and Power*, vol. 14, no. Nov, pp. 437–, 1968.

[5] A. L. Donaldson, "Electrode erosion in high current, high energy transient arcs," 1990.

[6] X. Zhou, J. Heberlein, and E. Pfender, "Theoretical-study of factors influencing arc erosion of cathode," *Ieee Transactions on Components Packaging and Manufacturing Technology Part A*, vol. 17, no. 1, pp. 107–112, 1994.

[7] J. J. Shea, "High current ac break arc contact erosion," in *Electrical Contacts, 2008. Proceedings of the 54th IEEE Holm Conference on*, pp. xxii–xlvi.

[8] G. R. Jones and P. C. Russell, "Chromatic modulation based metrology," *Pure and Applied Optics: Journal of the European Optical Society Part A*, vol. 2, no. 2, p. 87, 1993.

[9] L. T. Isaac, *Puffer circuit breaker diagnostics using novel optical fibre sensors*. Thesis, 1997.

[10] Z. Wang, J. W. Spencer, J. D. Yan, G. R. Jones, J. E. Humphries, M. Z. Wang, and X. H. Wang, "Preliminary spectroscopic investigation of hvcb contacts erosion," in *XXIst Symposium on Physics of Switching Arc*.

[11] P. Borkowski and E. Walczuk, "Temperature rise behind fixed polarity ag-w contacts opening on an half cycle of high current and its relationship to contact erosion," *Electrical Contacts-2004: Proceedings of the 50th Ieee Holm Conference on Electrical Contacts/the 22nd International Conference on Electrical Contacts*, pp. 334–340, 2004.

[12] NIST. http://www.nist.gov.

[13] G. R. Jones, A. G. Deakin, and J. W. Spencer, *Chromatic monitoring of complex conditions*. Series in sensors, CRC Press, 2008.

[14] Y. L. Wang, S. H. Liang, and Z. B. Li, "Experiment and simulation analysis of surface structure for cuw contact after arc erosion," *Materials Science and Technology*, vol. 31, no. 2, pp. 243–247, 2015.